Total Ozone From the Ozone Monitoring Instrument (OMI) Using the DOAS Technique

J. Pepijn Veefkind, Johan F. de Haan, Ellen J. Brinksma, Mark Kroon, and Pieternel F. Levelt

***Abstract*—This paper describes the algorithm for deriving the total column ozone from spectral radiances and irradiances measured by the Ozone Monitoring Instrument (OMI) on the Earth Observing System Aura satellite. The algorithm is based on the differential optical absorption spectroscopy technique. The main characteristics of the algorithm as well as an error analysis are described. The algorithm has been successfully applied to the first available OMI data. First comparisons with ground-based instruments are very encouraging and clearly show the potential of the method.**

***Index Terms*—Ozone, remote sensing, satellites applications, terrestrial atmosphere.**

I. Introduction

ON JULY 15, 2004, the Ozone Monitoring Instrument (OMI) onboard the National Aeronautics and Space Administration's (NASA) Earth Observing System (EOS) Aura satellite was launched. The OMI is the first of a new generation of spaceborne spectrometers that combine a high spatial resolution (13×24 km^2 at nadir) with daily global coverage [1]. Measuring the trend in stratospheric ozone as well as detecting tropospheric ozone on regional scales are top priorities among the science objectives for the Aura satellite [2].

Space-based measurements of the ozone column have been performed operationally since the 1970s with the Solar Backscatter Ultraviolet (SBUV) and Total Ozone Mapping Spectrometer (TOMS) series of instruments [3]. These measurements have played a major role in atmospheric chemistry, for example by monitoring the ozone layer [4], as a tracer for measuring stratospheric dynamics (e.g., see [5]), and by detecting tropospheric ozone pollution on a regional scale [6]. The original SBUV and TOMS instruments measure the backscattered radiance in a few 1-nm-wide bands. From these bands, the ozone column is derived using radiances measured at two wavelengths, while other wavelengths are used for diagnostics and error correction [7], [8]. In 1995 the Global Ozone Monitoring Experiment (GOME) instrument was launched as the first of a series of space instruments that measure the ultraviolet and visible part of the spectrum with a moderately high spectral resolution. In 2002 the SCIAMACHY instrument was launched, followed by OMI in 2004. These spectrometers make it possible to derive the ozone column using differential optical absorption spectroscopy (DOAS) [9]–[11], since they measure the entire Huggins ozone absorption bands continuously rather than just at a few wavelengths. DOAS was developed for ground-based measurements of atmospheric trace gases [12], [13], but can also be applied to measurements from space. DOAS derives the ozone column by fitting a reference ozone absorption cross section at the instrument's spectral resolution to the measured sun-normalized radiance. The main advantages of DOAS compared to the original SBUV/TOMS techniques are that DOAS is less sensitive to the radiometric calibration of the instrument and less sensitive to disturbing factors like absorbing aerosols, as it makes use of a relatively large absorption spectral range with several to many spectral features. In this paper the implementation of the DOAS technique for measuring total ozone is described. First results of applying the algorithm to OMI data are presented, as well as first comparisons with ground-based data.

Manuscript received April 29, 2005; revised October 14, 2005. This work was supported by the Netherlands Agency for Aerospace Programs (NIVR). The OMI instrument was contributed by The Netherlands (NIVR/KNMI) and Finland (TEKES/FMI) to the NASA EOS Aura mission.

The authors are with the Royal Netherlands Meteorological Institute (KNMI), De Bilt, The Netherlands (e-mail: veefkind@knmi.nl).

Digital Object Identifier 10.1109/TGRS.2006.871204

II. Algorithm Description

The OMI total ozone DOAS algorithm consists of three steps. First, the DOAS method is used to fit the differential absorption cross section of ozone to the measured sun-normalized Earth radiance spectrum, to obtain the so-called slant column density. In the second step the slant column density is translated into the vertical column density using the so-called air mass factor. The third step consists of a correction for cloud effects, to account for ozone that is obscured by clouds. In this section we describe these steps, including the physical background, as well as assumptions and *a priori* information on which the results depend.

A. Step 1: Deriving the Slant Column Density

The first step in the ozone DOAS algorithm is to determine the slant column density, which is defined as the amount of ozone along an average path taken by photons within a fit window as they travel from the sun, through the atmosphere to the satellite sensor. There are many paths that will contribute to the slant column density, involving scattering and absorption within the atmosphere as well reflection by the surface. The slant column density is determined by fitting a function to the ratio of the measured Earth radiance to the solar irradiance data. This fit is applied to data taken in a certain wavelength range, called the fit window. A polynomial function, which serves as a high-pass filter, is applied to account for scattering and absorption that vary gradually with the wavelength, e.g., reflection by the surface and scattering by molecules, aerosols, and clouds. Also, the high-pass filter takes out gradually varying radiometric calibration errors and other instrumental multiplicative effects. The

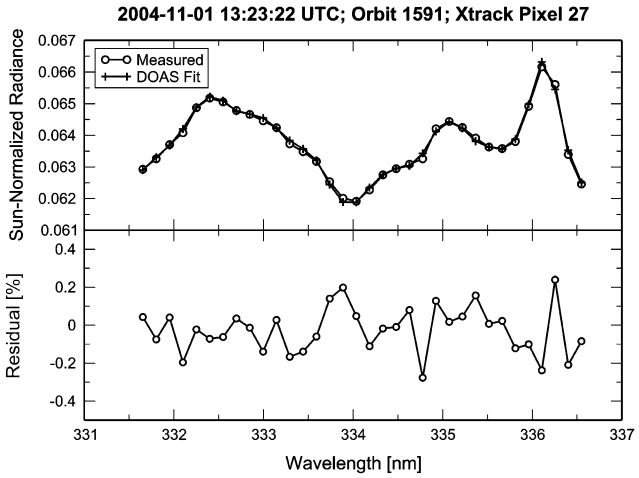

Fig. 1. Example of a DOAS fit on OMI data measured on November 1, 2004 13:23:32 UTC. (Upper panel) Measured sun-normalized radiance and the result of the DOAS fit. (Lower panel) Residual between measurement and fit, expressed as the relative difference between the two.

slant column density is derived from the filtered data, which contains spectral features of ozone and other molecules in the fit window. Fig. 1 shows a DOAS fit applied to OMI data. The fit function that is used in the OMI algorithm is based on the following equation:

$$\frac{I(\lambda)}{F(\lambda)} = P(\lambda)\exp[-N_s\sigma_{\mathrm{O3}}(\lambda, T_{\mathrm{eff}})] \tag{1}$$

where I is the radiance; F is the extraterrestrial solar irradiance; P is a low-order polynomial; N_s is the ozone slant column density; σ_{O3} is the absorption cross section of ozone; λ is the wavelength; and T_{eff} is the effective ozone temperature. To properly account for temperature effects the effective ozone temperature is derived from the DOAS fit itself. This is done by linearizing the cross section around a reference temperature T_0, thus writing the ozone absorption cross section in (1) as

$$\sigma_{\mathrm{O3}}(\lambda, T_{\mathrm{eff}}) = \sigma_{\mathrm{O3}}(\lambda, T_0) + (T_{\mathrm{eff}} - T_0)\left.\frac{d\sigma_{\mathrm{O3}}(\lambda)}{dT}\right|_{T=T_0}. \tag{2}$$

Equation (1) is only accurate when dealing with elastic scattering. However, approximately 6% of the light scattering events in the OMI fit window are inelastic, meaning that the scattered light is at a different wavelength than the incoming light. The effect of this inelastic rotational Raman scattering is that structures in the spectrum are reduced. This holds for Fraunhofer structures (the well-known Ring effect) as well as for spectral structures caused by absorption in the atmosphere. Because Raman scattering reduces spectral structures, not accounting for it properly can cause an underestimation of the slant column density of the order 3% to 10% [14]. When including terms that account for Raman scattering, the fit function can be expressed as

$$\frac{I(\lambda)}{F(\lambda)} = P(\lambda)\exp[-N_s\sigma_{\mathrm{O3}}(\lambda, T_{\mathrm{eff}})] + c_{\mathrm{Ring}}\frac{I_{\mathrm{Ring}}(\lambda)}{F(\lambda)}\exp[-N_s\sigma'_{\mathrm{O3}}(\lambda, T_{\mathrm{eff}})] \tag{3}$$

where I_{Ring} is the extraterrestrial solar irradiance convoluted with the Raman lines; c_{Ring} is fit parameter to scale the radiance due to Raman scattering and is determined from the depth of the Ring lines in the fit window; and σ'_{O3} is an effective ozone absorption cross section partly scrambled by rotational Raman scattering. Incident sunlight traveling through the atmosphere picks up absorption features of ozone. When rotational Raman scattering occurs these absorption features are convoluted with rotational Raman lines yielding scrambled absorption features. After the Raman scattering, light picks up ozone absorption features again, and the ozone signal at the detector is partly scrambled. This process can be described in terms of an effective cross section that is partly scrambled by Raman scattering. Detailed descriptions are given by [15] and [16].

The fit parameters of (3) ($N_s, T_{\mathrm{eff}}, c_{\mathrm{Ring}}$, and the polynomial coefficients) are determined using a nonlinear, least squares fit. Information on the quality of the fit and the fit parameters is derived from the associated covariance matrix. The reference ozone cross-sections were determined by convolving the spectrally recalibrated cross-sections of [17] and [18], with the OMI spectral response (slit function). In these convolutions the spectral features of the sun were accounted for (the so-called I_0 effect).

Detailed studies were performed to find the optimum fit window for ozone. The conclusions of these studies are that the main drivers for the fit window are the sensitivity of the slant column density to the atmospheric temperature and to the instrument signal-to-noise. The temperature effects are smallest in the parts of the spectrum where the correlation between the high-pass-filtered ozone cross section and its derivative to the temperature is minimal. The signal-to-noise effects put a lower limit on the width of the fit window. Based on these considerations a 5-nm-wide window centered around 334.1 nm was selected as the default fit window for OMI. For this fit window a second-degree polynomial is used as high-pass filter. Extension of the fit window toward smaller wavelengths has several consequences, such as a reduced sensitivity to instrumental noise, an increased sensitivity to the temperature profile, a reduced accuracy of the fit because DOAS becomes less accurate for stronger absorption, a slightly increased sensitivity for the ozone profile, and the requirement to go from a second-order polynomial to a third-order polynomial as high-pass filer. The sensitivity studies that were performed showed that some other windows give a good performance, but that the window selected is optimal for an OMI-like instrument for average conditions.

B. Step 2: Air Mass Factor Correction

In DOAS, the air mass factor is used to translate the slant column density into a vertical column density. The air mass factor M is defined as the ratio of the slant column density, N_s, and the vertical column density, N_v. From this definition it follows that M will depend on the viewing and solar geometry, the fit window used, the surface albedo, the surface pressure, the actual ozone profile, clouds, and aerosols, as they all affect the apparent slant column amounts of ozone. The air mass factor is computed by simulating the measured spectra and applying DOAS to this simulated spectrum. For the simulations of the measured OMI spectrum a radiative transfer model is

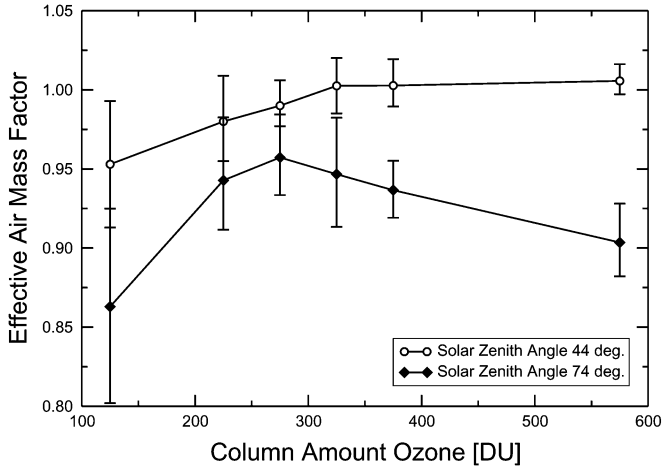

Fig. 2. Effective air mass factor (the air mass factor defined by the geometrical air mass factor) as a function of the total ozone column for two solar zenith angles. Each line shows the result of 648 profiles derived from the TOMS V8 ozone profile climatology. The symbols show the mean effective air mass factor at specific column amount ozone, and the bars show the minimum and maximum values. The solar zenith angles are 44° and 74°. The viewing angle is 33°. The relative azimuth angle is 90°, and the surface albedo is 0.1.

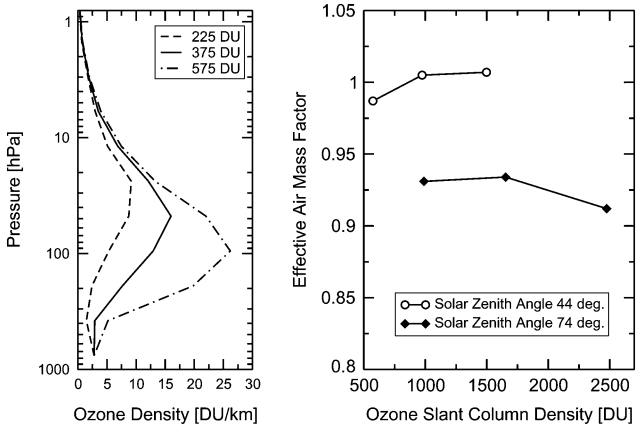

Fig. 3. (Left) Ozone profiles from the TOMS Version 8 climatology for 55° N for December, with a total column of ozone of 225, 375, and 575 DU. (Right) Effective air mass factors as a function of the slant column density for two sun–satellite geometries, as computed for the ozone profiles shown in the left panel. The sun–satellite geometries are: solar zenith angle 44° and 74°; viewing zenith angle 34°; and relative azimuth angle 90°. The surface albedo is 0.1.

used, in combination with a simple OMI simulator. The OMI simulator is used to translate the high-resolution spectra from the radiative transfer model into spectra at the OMI spectral resolution and sampling. On the simulated spectra, the DOAS fit function is applied to compute the slant column density. Since for the simulated spectra the vertical column density is known, the air mass factor can be computed as $M = N_s/N_v$. The calculated air mass factor is accurate if the model atmosphere used in the radiative transfer calculations resembles the actual atmosphere.

The air mass factor is precomputed and stored in lookup tables as a function of the sun–satellite geometry, the surface pressure and albedo, latitude, month, and total ozone amount. The surface pressure is derived from the altitude of the ground pixel, assuming a standard sea level pressure of 1013 hPa. The ozone profiles are based on the TOMS V8 ozone climatology [7]. The surface albedo is derived by combining the TOMS surface albedo climatology [19] with actual snow cover and sea ice coverage information. Fig. 2 shows the dependence of the air mass factor on the ozone profile, if no *a priori* information on the ozone profile shape were used. This figure shows that the dependence is largest for ozone hole conditions, whereas the dependence on Solar zenith angle is very weak. To reduce the uncertainty in the air mass factor due to the variations in the ozone profile, the appropriate profile is estimated based on the measured slant column density. To derive a relation between the slant column density and the ozone profile, three ozone profiles are used that cover the natural variability of the ozone profile for a given location and time period. For each of these profiles the slant column density and air mass factor is calculated for a given sun–satellite geometry, cloud condition, and surface property. In this manner a relationship is derived between the air mass factor and the slant column density, as illustrated in Fig. 3. The air mass factor to be applied to the measurement is computed by evaluating this relationship for the measured slant column density.

C. Step 3: Cloud Correction

When a ground pixel is completely or partly covered by clouds, the algorithm has to account for the effects of clouds. Two kinds of effects are accounted for: first, the effects of clouds on the air mass factor, and second, the effect that clouds obscure part of the ozone column for satellite instruments.

To calculate the air mass factor for cloudy conditions a cloud model is necessary. To determine the air mass factor for cloudy conditions, the cloud fraction and cloud pressure from the OMI O_2-O_2 cloud product are used [20]. For consistency, it is important to use the same cloud model as used in the cloud product. This cloud model represents clouds by opaque Lambertian surfaces with an albedo of 0.80, placed at the cloud pressure. It was found by [21] that this value for the cloud albedo gives the best results for ozone retrieval using DOAS. This cloud model considers all clouds to be thick, single layer clouds. Partly cloudy pixels are treated as the weighted sum of a clear and a cloudy pixel. Pixels that are fully covered with thin clouds are represented by partly cloudy pixels with a thick cloud. Using this cloud model, the air mass factors for fully cloudy conditions are determined in the same manner as those for clear ground pixels described in the previous section, but with a Lambertian surface of albedo 0.80 at the cloud pressure level. Partly cloudy ground pixels are treated as the weighted sum for clear and cloudy conditions

$$M = w \cdot M_{\text{cloudy}} + (1 - w) M_{\text{clear}}. \tag{4}$$

where the weight w is the fraction of the radiance that is due to the cloudy part of the ground pixel.

The amount of ozone below the Lambertian cloud is called the "ghost column" and is computed by integrating the ozone profile from the surface to the cloud pressure. The profiles are taken from the TOMS V8 climatology [7]. Just as for the air mass factor, the appropriate profile, and hence, the appropriate ghost column is estimated using the measured slant column density.

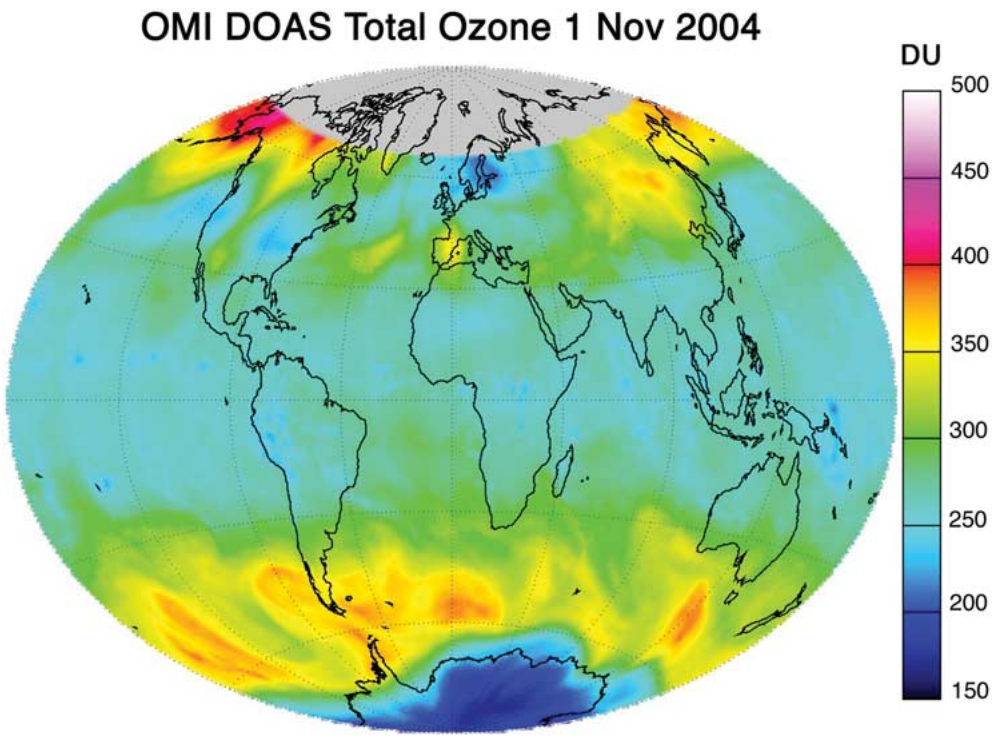

Fig. 4. Total ozone column for November 1, 2004, derived using the OMI DOAS algorithm.

Finally, the vertical column amount N_v can be computed

$$N_v = \frac{N_s + w \cdot M_{\text{cloudy}} \cdot N_g}{M} \tag{5}$$

where N_g is the ghost column.

III. Error Analysis

During the development phase of the algorithm an extensive error analysis was performed to estimate the expected accuracy of the algorithm [22]. The focus of this error analysis was on nominal cases. Exceptional cases, such as, for example, desert dust and polar stratospheric clouds, were assessed separately. Table I summarizes the results from the error analysis for each of the algorithm steps (slant column density, air mass factor, and cloud correction), as well as for the vertical column density. In this table, a distinction is made between the total and the relative error. The relative errors are defined as errors that can vary for two measurements for the same location for two successive days. Thus, the systematic errors, which are not important for deriving trends, are excluded from the relative error. As can be seen in Table I, the relative error of the vertical column density is 1.3% for a cloud-free pixel, 2.2% for a cloudy pixel, and 1.7% for a partly cloudy pixel. For cloudy conditions, the relative error is dominated by errors in the air mass factor related to clouds, whereas for cloud-free conditions, it is dominated by the instrument signal to noise. If one is interested in trends, it seems best to focus on cloud-free conditions. Then random errors, e.g., instrument noise, will average out. The error that dominates for trend analysis is then a bias in the assumed ozone profile.

TABLE I
Error Estimates for the OMI Ozone DOAS Product. Errors Ordered According to the Three Algorithm Steps: Slant Column Density, Air Mass Factor, and Cloud Correction, As Well As for the Resulting Error on the Total Column Ozone

	Total Error [%]	Relative Error [%]
Errors on the Slant Column Density:		
Other trace gases	0.5	0.5
Absorption cross-section	1	
Instrument spectral response function (slit function)	0.1	
Atmospheric temperature	0.3	0.3
Instrument signal-to-noise	1	1
Instrument spectral calibration	1	
Instrument spectral stability[a]	0.25	
Errors on the Air mass factor:		
Aerosols	0.2	0.2
Cloud Model	1	1
Ozone profile	0.5	0.5
Surface reflectivity	0.3	
Cloud pressure	1	1
Cloud fraction	0.8	0.8
Errors on the Cloud Correction ghost column[b]	40	40
Resulting Errors on the Vertical Column Density:		
Clear	2.1	1.3
Partly Cloudy	2.5	1.7
Cloudy	3.0	2.2

[a] Spectral stability over a typical time period of one day.
[b] Generally the ghost column is no more than a few percent of the total column. A 40 % error in the ghost column contributes little to the error in the total column.

IV. First Results

From the beginning of October until the end of November 2004, OMI measured the Earth radiance almost continuously.

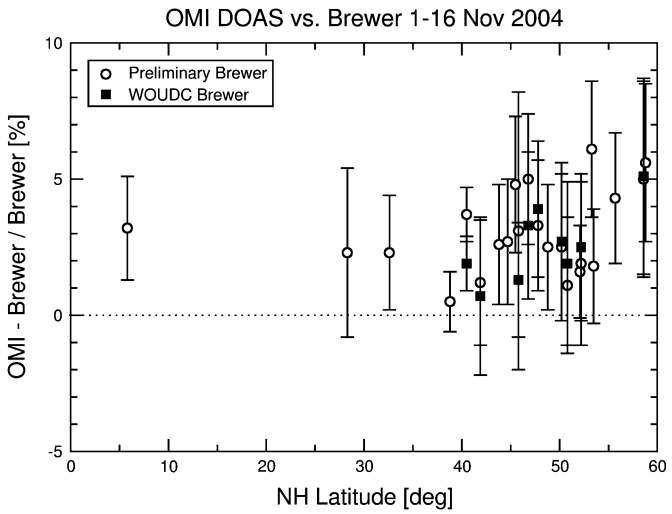

Fig. 5. Comparisons between the OMI total ozone column from the DOAS algorithm and available Brewer stations in the Northern Hemisphere, for the period November 1–16 , 2004. Filled squares are used from Brewer data from the WOUDC. Open circles are used for preliminary (quick-look) Brewer data. OMI data points colocated within 50 km and 1 h are included in this figure.

This time period covers an important part of the Antarctic ozone hole for that year. Fig. 4 shows an example of the total ozone derived for November 1, 2004, clearly showing the Antarctic ozone hole. This figure also illustrates the daily global coverage of the OMI instrument. To make a first assessment of the quality of the ozone data from the algorithm, a comparison was performed with available Brewer stations in the Northern Hemisphere. It is noted that this exercise is the very beginning of the validation effort. As described in [23], the core validation will include many more comparisons with all sorts of correlative data. The first comparisons show that the average bias of the OMI DOAS total ozone, as compared with the Brewer results, is $2.9 \pm 2.5\%$, see Fig. 5. The OMI data seem to be slightly higher than the Brewer observations. Although the reported difference is of the order of the expected accuracy, we believe that further improvement is possible. Apart from improvements in the (spectral) calibration of the instrument, improvements in the cloud correction part will become possible if better estimates of the cloud fraction become available. Also we expect that the Brewer data become better when the final data for all locations can be used.

V. Conclusion

In this paper, the DOAS algorithm for deriving the total ozone column from OMI data was described, and first results are presented. First comparisons with ground-based observations for the Northern Hemisphere for a limited time period, show agreement within 3%. This is of the same order of magnitude as expected from an error analysis. However, significant improvement of the OMI total ozone product is expected.

Acknowledgment

The authors wish to thank the Principal Investigator's of each contributing Brewer station for providing their preliminary total ozone data for OMI validation and D. Balis (Aristotle University of Thessaloniki) for making the Brewer ozone data available to us.

References

[1] P. F. Levelt, G. H. J. van den Oord, M. R. Dobber, A. Mälkki, H. Visser, J. de Vries, P. Stammes, J. Lundell, and H. Saari, "The Ozone Monitoring Instrument," *IEEE Trans. Geosci. Remote Sens.*, vol. 44, no. 5, pp. 1093–1101, May 2006.

[2] P. F. Levelt, E. Hilsenrath, G. W. Leppelmeier, G. B. J. van den Oord, P. K. Bhartia, J. Tamminen, J. F. de Haan, and J. P. Veefkind, "Science objectives of the Ozone Monitoring Instrument," *IEEE Trans. Geosci. Remote Sens.*, vol. 44, no. 5, pp. 1199–1208, May 2006.

[3] D. F. Heath and H. Park, "The solar backscatter ultraviolet (SBUV) and Total Ozone Mapping Spectrometer (TOMS) experiment," in *The Nimbus-7 Users Guide*, C. R. Madrid, Ed. Greenbelt, MD: NASA Goddard Space Flight Center, 1978, pp. 175–211.

[4] M. P. Chipperfield *et al.*, "Global ozone past and future," in *Scientific Assessment of Ozone Depletion: 2002*. Geneva, Switzerland: WMO, Mar. 2003, pp. 4.1–4.90.

[5] W. Steinbrecht, H. Claude, U. Köhler, and K. P. Hoinka, "Correlations between tropopauuse height and total ozone: Implications for long-term changes," *J. Geophys. Res.*, vol. 103, no. D5, pp. 19 183–19 192, 1998.

[6] J. Fishman, C. E. Watson, J. C. Larsen, and J. A. Logan, "Distribution of tropospheric ozone determined from satellite data," *J. Geophys. Res.*, vol. 95, pp. 3599–3617, 1990.

[7] P. K. Bhartia and C. Wellemeyer, "TOMS-V8 total O3 algorithm," NASA Goddard Space Flight Center, Greenbelt, MD, OMI Alg. Theoret. Basis Doc., OMI Ozone Product OMI-ATBD-02, vol. II, P. K. Bhartia, Ed., 2002.

[8] P. K. Bhartia, R. D. McPeters, L. E. Flynn, and C. G. Wellemeyer, "Highlights of the version 8 SBUV and TOMS datasets released at this symposium," in *Proc. Quad. Ozone Symp.*, C. Zerefos, Ed., Athens, Greece, 2004, p. 294.

[9] R. Spurr, "GOME Level 1 to 2 algorithms description," DLR, Oberpfaffenhofen, Germany, Tech. Note ER-TN-DLR-GO-0025, 1994.

[10] J. P. Burrows, M. Weber, M. Buchwitz, V. Rozanov, A. Ladstätter-Weissenmayer, A. Richter, R. De Beek, R. Hoogen, K. Bramstedt, K. W. Eichmann, M. Eisinger, and D. Perner, "The Global Ozone Monitoring Experiment (GOME): Mission concept and first scientific results," *J. Atmos. Sci.*, vol. 56, pp. 151–175, 1999.

[11] A. J. M. Piters, P. J. M. Valks, R. B. A. Koelemeijer, and D. M. Stam, "GOME ozone fast delivery and value-added products, version 3.0," KNMI, De Bilt, The Netherlands, Rep. GOFAP-KNMI-ASD-01, 2000.

[12] J. F. Noxon, "Nitrogen dioxide in the stratosphere and troposphere measured by ground-based absorption spectroscopy," *Science*, vol. 189, no. 547, 1975.

[13] U. Platt, "Differential optical absorption spectroscopy (DOAS)," in *Air Monitoring by Spectroscopic Techniques*, M. W. Sigrist, Ed. New York: Wiley, 1994, pp. 27–84.

[14] P. J. M. Valks, "Retrieval of total and tropospheric ozone from observations by the Global Ozone Monitoring Experiment," Ph.D. dissertation, Dept. Phys., Eindhoven Tech. Univ., Eindhoven, The Netherlands, 2003.

[15] J. F. de Haan, "Accounting for Raman scattering in DOAS, version 1.0," KNMI, De Bilt, The Netherlands, Tech. Note SN-OMI-KNMI-409, 2003.

[16] H. J. Eskes, R. J. van der A, E. J. Brinksma, J. P. Veefkind, and J. F. de Haan, "Retrieval and validation of ozone columns derived from measurments of SCIAMACHY on Envisat," *Atmos. Chem. Phys. Discuss.*, vol. 5, pp. 4429–4475, 2005.

[17] A. M. Bass and R. J. Paur, "The ultraviolet cross-sections of ozone. I. The measurements. II—Results and temperature dependence," in *Proc. Quad. Ozone Symp.*, C. Zefros and A. Ghazi, Eds., Dordrecht, The Netherlands, 1986, p. 606.

[18] J. Orphal and K. Chance, "Ultraviolet and visible absorption cross-sections for HITRAN," *J. Quant. Spectrosc. Radiat. Transf.*, vol. 82, pp. 491–504, 2003.

[19] J. R. Herman and E. A. Celarier, "Earth surface reflectivity climatology at 340–380 nm from TOMS data," *J. Geophys. Res.*, vol. 102, pp. 28 003–28 011, 1997.

[20] J. R. Acarreta, J. F. de Haan, and P. Stammes, "Cloud pressure retrieval using the O2–O2 absorption band at 477 nm," *J. Geophys. Res.*, vol. 109, no. D05204, 2004.

[21] R. B. A. Koelemeijer and P. Stammes, "Effects of clouds on ozone column retrieval from GOME UV measurements," *J. Geophys. Res.*, vol. 104, no. D7, pp. 8281–8294, 1999.

[22] J. P. Veefkind and J. F. de Haan, "DOAS total O3 algorithm," NASA Goddard Space Flight Center, Greenbelt, MD, OMI Alg. Theoret. Basis Doc., OMI Ozone Product OMI-ATBD-02, vol. II, P. K. Bhartia, Ed., 2002.

[23] E. J. Brinksma and R. McPeters, "Ozone column workpackage, in *Ozone Monitoring Instrument Detailed Validation Handbook*," KNMI, De Bilt, The Netherlands, Tech. Note TN-KNMI-OMIE-583, M. Kroon and E. J. Brinksma, Eds., 2004.

J. Pepijn Veefkind is an expert in the field of satellite remote sensing of aerosols and trace gases. He has experience in developing and validating retrieval algorithms for satellite based radiometers and spectrometers. During his Ph.D. research, he developed different techniques for the retrieval of aerosol optical thickness from GOME, ATSR-2, and AVHRR data and participated in several international field experiments. Since 1999, he has been working in the Ozone Monitoring Instrument (OMI) PI Team, which is part of the Atmospheric Composition Division, Royal Dutch Meteorological Institute (KNMI), De Bilt, The Netherlands. He is responsible for the development and implementation of retrieval algorithms for the OMI ozone column, ozone profile, NO_2, aerosol, and cloud products. He is chairing the Algorithms Working Group of the International OMI Science Team. His research interests include retrieval techniques, global monitoring of aerosols and trace gases, intercomparison of satellite measurements from different sensors, radiative forcing of climate, and satellite detection of air pollution.

Johan F. de Haan received the M.S. degree in physics and the Ph.D. degree from the Free University of Amsterdam, Amsterdam, The Netherlands, in 1978 and 1987, respectively. His Ph.D. thesis, entitled "Effects of aerosols on the brightness and polarization of cloudless planetary atmospheres" was defended successfully in 1987 (promoter: Prof. Dr. J. W. Hovenier). The thesis deals with the development of an improved adding/doubling code to calculate the degree of polarization of sunlight scattered by the atmospheres of the Earth and Mars. The code was applied to these atmospheres and effects of aerosols on the scattered light were investigated.

Between 1987 and 2003, he was involved in educating Ph.D. students in the Astronomy Department, Free University. He worked together with Ph.D. students on diverse subjects, such as light scattering by nonspherical aerosol particles, and the interpretation of measurements of polarized light scattered by the atmospheres of the Earth, Venus, and Jupiter. Between 1994 and 2000, he worked part-time at the Survey Department of Rijkswaterstaat, Delft, The Netherlands, on the interpretation of remote sensing images of coastal and inland waters. This included the development and application of schemes for atmospheric correction of those images and the improvement of retrieval algorithms for chlorophyll, suspended sediment, and yellow substance. In 2000, he began work at KNMI on OMI retrieval algorithms. He developed a scheme to improve the correction for rotational Raman scattering in the total ozone DOAS algorithm, thereby eliminating errors in the total ozone column of up to 10%. Currently, he is responsible for the OMI ozone profile algorithm, which is being extended to include rotational Raman scattering. Further, he is involved in the OMI cloud retrieval algorithm and is investigating ways to improve the current algorithm that is based on absorption by the O_2-O_2 collision complex at 477 nm. In general, specialized knowledge on radiative transfer and a good overall knowledge of numerical techniques are used to extend and improve retrieval algorithms. Special care is taken to ensure that the physics behind the algorithms is sound.

Ellen J. Brinksma studied astrophysics and received the Ph.D. degree in lidar studies of the middle atmospere from Vrije Universiteit, Amsterdam, The Netherlands, in 2001.

In January 2000, she joined the OMI Science Team at the Royal Netherlands Meteorological Institute (KNMI), De Bilt, where she works on satellite validation, satellite retrievals, and ground-based measurements, with a focus on ozone and nitrogen dioxide. She has published 15 peer-reviewed papers on atmospheric science topics.

Mark Kroon studied experimental laser physics at the University of Amsterdam, Amsterdam, The Netherlands, and the Ph.D. degree in the field of phase transitions in soft condensed matter from the University of Amsterdam in 1998.

He was with Philips Research Laboratories where he worked in the field of optical microlithography. In January 2003, he joined the OMI Team at the Royal Netherlands Meteorological Institute, De Bilt, on the position of Validation Work Package Leader, coordinating the international efforts for the validation of all OMI data products.

Pieternel F. Levelt received the M.S. degree in physical chemistry and the Ph.D. degree from the Free University of Amsterdam, Amsterdam, The Netherlands, in 1987 and 1992, respectively. Her Ph.D. work consisted of the development of a XUV spectrometer-based nonlinear optical technique and performing XUV spectroscopy on small diatomic molecules.

In 1993, she started working at the Royal Netherlands Meteorological Institute (KNMI), De Bilt, in the Atmospheric Composition section at the Research Department of KNMI. There, she worked on chemical data assimilation of ozone in two-dimensional and three-dimensional chemistry transport models and on the validation of the European satellite instruments GOME and SCIAMACHY. She was a Member of the Algorithm and Validation subgroups of GOME and SCIAMACHY. She was strongly involved in the validation program of both instruments. Since July 1998, she has been Principal Investigator of the OMI instrument and is responsible for the scientific program of OMI and managing the international OMI Science Team. She is also the Project Manager of the OMI Program at KNMI and responsible for the development of algorithms, validation, and data processing of OMI products and in-flight calibration and operational planning of the OMI instrument. She is managing the OMI team at KNMI consisting of 15 to 35 people. As Principal Investigator, she is advising NIVR on OMI instrument requirements and performance.